

Control of blood and gas pressure dynamics in a mathematical model of the cardiovascular-respiratory system for maintaining homeostasis during exercise in Chad

Guibé Séhoré^{1,*}, Jean Marie Ntaganda², Ngarkodje Ngarasta³

¹Department of Mathematics, University of N'Djamena, Chad
g.sehore91@gmail.com

²Department of Mathematics, College of Science and Technology,
University of Rwanda, Rwanda
jmnta@yahoo.fr

³Department of Mathematics, University of Sarh, Chad
ngarkodje@yahoo.fr

Received: 3 October 2025, Published: 27 March 2026

Abstract: This study develops an integrated mathematical model of the cardiovascular-respiratory system to investigate the regulation of blood and gas pressure dynamics during physical exercise in a Chadian athletic population. Heart rate and alveolar ventilation are incorporated as control inputs within an optimal control framework to explain the stabilization of systemic arterial pressure (P_{as}), systemic venous pressure (P_{vs}), and arterial partial pressures of oxygen (P_{aO_2}) and carbon dioxide (P_{aCO_2}) during moderate and intense exercise. The model is calibrated using field data collected from elite male and female football players and discretized using B-spline basis functions to compute optimal control trajectories.

Simulation results show a strong concordance between the measured physiological variables and the model predictions, as confirmed by the RMSE and MAE values reported in Tables 7 and 8. Moreover, clear sex-related ventilatory differences emerge from the simulations: under comparable exercise intensity, male and female athletes exhibit a measurable gap in alveolar ventilation, with a difference quantified as $\Delta\dot{V}_A = 1.8 \text{ L} \cdot \text{min}^{-1}$.

The objective of this modeling approach is primarily explanatory rather than predictive, aiming to reproduce and interpret the physiological mechanisms governing cardiorespiratory adaptation to exercise rather than to provide long-term individual predictions. The proposed framework demonstrates the capacity of optimal control-based models to capture realistic, population-specific cardiorespiratory responses and provides a foundation for future refinement and validation using larger experimental datasets.

Keywords: heart rate, alveolar ventilation, blood pressures, gas pressures, mathematical model, Chad

I. INTRODUCTION

The cardiovascular and respiratory systems work in tandem to maintain homeostasis, particularly by regulating blood pressure and gas exchange, which are vital during physical exertion. Heart rate and alveolar ventilation serve as primary physiological control

Copyright: © 2026 Guibé Séhoré, Jean Marie Ntaganda, Ngarkodje Ngarasta. This article is distributed under the terms of the Creative Commons Attribution License (CC BY 4.0), which permits unrestricted use, distribution, and reproduction in any medium, provided the original author and source are credited.

*Corresponding author

Citation: Guibé Séhoré, Jean Marie Ntaganda, Ngarkodje Ngarasta, Control of blood and gas pressure dynamics in a mathematical model of the cardiovascular-respiratory system for maintaining homeostasis during exercise in Chad, Biomath 15 (2026), 2603274, <https://doi.org/10.55630/j.biomath.2026.03.274>

mechanisms to modulate cardiac output and pulmonary gas exchange, thereby stabilizing systemic arterial pressure (P_{as}), systemic venous pressure (P_{vs}), and arterial partial pressures of oxygen (P_{aO_2}) and carbon dioxide (P_{aCO_2}). During exercise, oxygen demand increases substantially, inducing marked cardiovascular and respiratory adaptations that challenge the stability of these pressure dynamics [1]. Developing mathematical models capable of representing such dynamics is therefore essential for understanding physiological regulation and for designing effective control strategies to preserve homeostasis during exercise, particularly within specific and underrepresented populations such as those in Chad.

Exercise induces complex and nonlinear changes in cardiovascular and respiratory function. Increased metabolic demand elevates cardiac output through coordinated adjustments in heart rate and stroke volume, while ventilation increases to satisfy oxygen uptake and facilitate carbon dioxide elimination [2]. The interaction between these systems results in highly dynamic pressure responses that require precise regulation to avoid physiological imbalance. Mathematical modeling of these coupled processes provides a valuable framework for simulating exercise-induced responses and for evaluating control approaches aimed at optimizing physiological outcomes [3].

Mathematical modeling of the cardiovascular-respiratory system has progressed considerably over recent decades. Early work by Milhorn et al. [4] laid the foundation for respiratory control modeling through feedback regulation of blood gases. Subsequent studies incorporated cardiovascular dynamics to investigate the interplay between heart rate, ventilation, and vascular resistance [5]. Many of these models employ optimal control theory to adjust heart rate and ventilation in real time, thereby ensuring arterial pressure stability and gas exchange homeostasis under varying physiological conditions [6]. Batzel et al. [7] further demonstrated the effectiveness of optimal control strategies in integrated cardiorespiratory models, highlighting their relevance for exercise scenarios characterized by rapid and significant perturbations.

Despite these advances, existing integrated cardiorespiratory models are largely developed and validated using data from non-African populations and typically rely on generic parameter sets. In contrast, the present study introduces a localized modeling framework based on experimental data collected from elite Chadian football players, a population that remains largely underrepresented in physiological modeling

studies. The model incorporates sex-specific parameterization to capture physiological differences between male and female athletes and employs a numerical discretization of the optimal control problem using B-spline basis functions. This combination of population-specific data, sex-dependent calibration, and spline-based control discretization constitutes the principal novelty of the present work relative to previous integrated cardiovascular-respiratory models.

Chad presents specific challenges related to cardiovascular and respiratory health during physical activity. Environmental factors such as altitude and climate, combined with limited healthcare infrastructure and the prevalence of non-communicable diseases including hypertension and respiratory disorders, influence cardiorespiratory responses to exercise [8]. Moreover, daily activities and sporting practices often involve substantial physical exertion, making the understanding of exercise-induced pressure dynamics particularly relevant. Developing a region-specific mathematical model that accounts for these physiological and environmental factors is therefore essential for improving health assessment and guiding intervention strategies in the Chadian context.

The objective of this study is to develop a comprehensive mathematical model of the cardiovascular-respiratory system tailored to the Chadian population, with a particular focus on the control of pressure dynamics during exercise. The modeling framework adopts a primarily explanatory, rather than predictive, perspective, aiming to reproduce and interpret the physiological mechanisms governing cardiorespiratory regulation in response to exercise-induced perturbations. Heart rate and alveolar ventilation are introduced as control inputs to regulate systemic arterial and venous pressures, as well as arterial blood gas levels. By simulating exercise-induced disturbances, the proposed model enables the evaluation of optimal control strategies designed to maintain homeostasis and prevent maladaptive physiological responses.

This approach builds upon and extends previous modeling efforts. Magosso and Ursino demonstrated the capacity of mathematical models to capture cardiovascular responses to exercise and emphasized the role of feedback mechanisms [2]. Olufsen and Ottesen proposed patient-specific modeling frameworks combining cardiovascular and respiratory control with optimal control theory [5]. Cheng et al. [3] highlighted the influence of cardiorespiratory coupling on pressure variability. These studies inform the development of the present framework, which integrates local physiological

characteristics and environmental conditions relevant to Chad.

In summary, this paper presents a mathematical modeling and optimal control framework for analyzing cardiovascular-respiratory pressure regulation during exercise in a Chadian population. By combining population-specific data, sex-dependent parameterization, and spline-based numerical discretization, the proposed model provides a valuable tool for improving the understanding of exercise physiology and for supporting future physiological and clinical investigations in this context. The remainder of the paper is organized as follows: Section 2 describes the methodology and model formulation; Section 3 presents the optimal control problem; Section 4 details the numerical discretization; Section 5 reports the simulation results; Section 6 discusses the findings and their implications; and Section 7 concludes the study.

II. METHODS AND MATERIAL

A. Data source

The dataset used to calibrate and validate the cardio-respiratory model was collected from a cohort of 23 elite Chadian football players, including 11 men and 12 women, all competing professionally in the national first division. The athletes were in excellent health during the entire data collection period, with no reported medical conditions that could influence cardiovascular or respiratory responses. The average age of the male group was approximately 21 ± 3 years, while the female group had a mean age of around 24 ± 4 years.

All measurements were carried out at Paris-Congo Stadium in N'Djamena, located at an altitude of 295 meters. Training sessions took place during the early morning to ensure stable environmental conditions, with ambient temperatures ranging between 22°C and 25°C throughout the data collection period. Each athlete completed 15 structured training sessions lasting about two hours, during which physiological parameters were recorded twice per session: once at rest before exercising and once immediately after the training session, in order to capture the acute cardio-respiratory response to exercise.

To ensure consistency and accuracy, standardized procedures were applied across all sessions. Blood pressure was measured on the left arm using calibrated sphygmomanometers, while heart rate was recorded with cardiac monitors. Body weight and height were obtained using professional-grade scales and stadiometers; body temperature was measured with clinical thermometers; ambient temperature was recorded with

environmental thermometers; and altitude was assessed with digital altimeters. The athletes remained seated and relaxed during resting measurements to minimize variability.

Although the dataset includes detailed physiological information, the data remain confidential. Only anonymized, aggregated summaries were used for the modeling and analysis performed in this study.

The study was conducted in accordance with the ethical principles of the Declaration of Helsinki (World Medical Association, 2013) for research involving human subjects. The research protocol, including all procedures for physiological measurements and data collection, was reviewed and approved by the Ethics Committee of the Faculty of Science, University of N'Djamena, under reference number 261/PR/PM/MESRSFP/SE/SG/ASE/UDS/SG/2024. All participants were informed about the objectives and procedures of the study, as well as the potential risks associated with physical exercise. Each provided written informed consent prior to participation. The data collected were processed anonymously and confidentially, and used solely for scientific purposes.

Data availability: The individual raw physiological data used in this study are confidential and cannot be publicly shared. Anonymized and aggregated data supporting the findings of this study, as well as the model code, are available from the corresponding author upon reasonable request.

B. Mathematical model equations

The system dynamics are described by the mathematical model, expressed in the form of the following system of ordinary differential equations:

$$\begin{aligned} \tau_c \frac{dQ_c(t)}{dt} &= -Q_c(t) + \gamma_{Q_c} C_{vO_2}(t) W_r e^{T_{Dc}}, \\ \tau_{O_2} \frac{dQ_{O_2}(t)}{dt} &= -Q_{O_2}(t) + \gamma_{Q_{O_2}} C_{MLa}(t) W_r e^{T_{DO_2}}, \\ \rho \frac{dQ_{CO_2}(t)}{dt} &= -Q_{CO_2}(t) + \gamma_{Q_{CO_2}} C_{vO_2}(t), \\ V_M \frac{dC_{MLa}(t)}{dt} &= -C_{MLa}(t) + \gamma_{MLa} P_{aO_2}(t), \\ \frac{dC_{vO_2}(t)}{dt} &= -C_{vO_2}(t) + \gamma_{vO_2} Q_{O_2}(t) \\ \tau_E \frac{dV_E(t)}{dt} &= -V_E(t) + \gamma_{V_E} C_{MLa}(t) e^{T_{DE}}, \\ \frac{dP_{aO_2}(t)}{dt} &= -P_{aO_2}(t) + \gamma_{aO_2} P_{aCO_2}(t), \end{aligned}$$

Parameter	Description	Unit
Q_c	Cardiac output	$L \cdot \text{min}^{-1}$
Q_{O_2}	The oxygen extraction of the muscle	$\text{mL } O_2/\text{dl blood}$
Q_{CO_2}	Muscle carbon dioxide production	$L \cdot \text{min}^{-1}$
C_{MLa}	The lactate concentrations in the muscle compartment	mmol/L
C_{vO_2}	The concentration of oxygen in the mixed-venous blood entering the lung	$\text{mL } O_2/\text{dl blood}$
V_E	The pulmonary ventilation for a step increase of exercise	$L \cdot \text{min}^{-1}$
P_{aO_2}	Arterial oxygen partial pressure	mmHg
P_{aCO_2}	Arterial carbon dioxide partial pressure	mmHg
P_{as}	Systemic arterial blood pressure	mmHg
P_{vs}	Systemic venous blood pressure	mmHg

Table 1: Model variables.

$$\begin{aligned} \frac{dP_{aCO_2}(t)}{dt} &= -P_{aCO_2}(t) + \gamma_{aCO_2}P_{aO_2}(t), \\ \frac{dP_{as}(t)}{dt} &= -P_{as}(t) + P_{vs}^\alpha(t)f_1(H(t)), \\ \frac{dP_{vs}(t)}{dt} &= -P_{vs}(t) + P_{as}^\beta(t)f_2(\dot{V}_A(t)). \end{aligned} \quad (1)$$

Model parameter estimation was formulated within the optimal control framework as a constrained nonlinear optimization problem. The objective function consisted of a least-squares criterion quantifying the discrepancy between experimental measurements and simulated outputs of systemic arterial pressure (P_{as}), systemic venous pressure (P_{vs}), arterial oxygen partial pressure (P_{aO_2}), and arterial carbon dioxide partial pressure (P_{aCO_2}).

The parameter estimation problem was formulated as a constrained nonlinear optimization and solved using a Sequential Quadratic Programming (SQP) algorithm, implemented in the MATLAB environment through the `fmincon` function. The initial parameter values, reported in Table 4, were selected based on reference physiological models and data from the literature. Lower and upper bounds were imposed on each parameter to ensure physiological plausibility and numerical stability of the optimal control problem.

The Table 1 describes the variables of the mathematical model and their units. The model parameters, γ_{Q_c} , $\gamma_{Q_{O_2}}$, $\gamma_{Q_{CO_2}}$, γ_{MLa} , γ_{vO_2} , γ_{V_E} , γ_{aO_2} , γ_{aCO_2} , T_{Dc} , T_{DE} , T_{DO_2} , k_1 , k_2 , α and β are estimated and presented in Table 2, while those obtained from the literature are listed in Table 3.

In (1), the logistic functions f_1 and f_2 are formulated as follows.

$$\begin{aligned} f_1(H(t)) &= \frac{C_1 f_{1,0}}{f_{1,0} + (C_1 - f_{1,0}) e^{k_1 H(t)}}, \\ f_2(\dot{V}_A(t)) &= \frac{C_1 f_{2,0}}{f_{2,0} + (C_2 - f_{2,0}) e^{k_2 \dot{V}_A(t)}} \end{aligned}$$

where k_1 and k_2 represent the maximum growth rates of alveolar ventilation and heart rate, respectively, while C_1 and C_2 denote the maximum sustainable capacities for alveolar ventilation and heart rate, respectively. The constants $f_{1,0}$ and $f_{2,0}$ refer to the values of $f_1(H(t))$ and $f_2(\dot{V}_A(t))$ at the start of the evolutionary process.

The functions f_1 and f_2 model time-dependent control mechanisms in the cardiovascular-respiratory system. Depending on heart rate H and alveolar ventilation \dot{V}_A , they ensure a dynamic coupling between the cardiac and respiratory subsystems. Their logistic form captures the nonlinear and saturating nature of physiological regulation, guaranteeing bounded responses and a smooth convergence of the system toward equilibrium.

The inspiratory reserve volume (IRV) and expiratory reserve volume (ERV) are well-documented parameters in the scientific literature. Vital capacity (VC) can be estimated using predictive equations that account for individual factors such as sex, height (h), and age (a). According to [10], these relationships are expressed as follows:

$$\begin{aligned} VT &= VC - IRV - ERV, \\ VC^{male} &= (27.63 - 0.112a)h, \\ VC^{female} &= (21.78 - 0.101a)h, \end{aligned}$$

where VT denotes tidal volume. In addition, the predictive equations for systemic arterial pressure and systemic venous pressure are given as follows [12, 13]:

$$\begin{aligned} P_{as} &= P_{dias} + \frac{1}{3}(P_{sys} - P_{dias}), \\ P_{vs} &= P_{as} + Q \times R_s, \end{aligned}$$

The ratio between tidal volume (VT) and dead space volume (VD) provides an estimate based on a graphical analysis of the experimental data obtained during moderate exercise, as reported in [14] (Figures 17–18,

p. 82). This estimate can be expressed by the following relationship:

$$VD/VT = \frac{0.5578}{V_E} + 0.1482.$$

Under moderate exercise intensity, cellular oxygen utilization (Q_{O_2}) can be represented by a first-order linear dynamic model. The time constant associated with this process is close to that observed for systemic oxygen uptake (\dot{V}_{O_2}) [15–17]. Once physiological equilibrium is reached, both systemic oxygen uptake (\dot{V}_{O_2}) and cellular oxygen utilization (Q_{O_2}) vary proportionally with the mechanical power output (W_r). This dependence is commonly expressed as:

$$\Delta \dot{V}_{O_2} = 10 \times W_r,$$

where $\Delta \dot{V}_{O_2}$ denotes the increase in oxygen consumption (mL/min), while W_r refers to the work rate expressed in watts [17–19].

Furthermore, the partial pressures of oxygen and carbon dioxide in arterial blood can be expressed as follows [20, 21]:

$$P_{aCO_2} = \frac{863\dot{V}_{CO_2}}{V_E(1 - VD/VT)},$$

$$P_{aO_2} = 147 - \frac{863\dot{V}_{O_2}}{V_E(1 - VD/VT)}.$$

At rest, the heart provides a total cardiac output of approximately $5 \text{ L} \cdot \text{min}^{-1}$, with around $0.75 \text{ L} \cdot \text{min}^{-1}$ directed to the muscles. During physical exertion, the increase in cardiac output is generally assumed to be entirely redirected to the active muscles [22], as illustrated by the following equation:

$$Q_c = 0.05W_r + 5.$$

III. FORMULATION AND DISCRETIZATION OF OPTIMAL CONTROL PROBLEM

To formulate the optimal control problem, we define the state vector $X = (P_{aO_2}, P_{aCO_2}, P_{as}, P_{vs})^t$, representing the key physiological variables to be regulated. These include arterial partial pressures of oxygen and carbon dioxide, systemic arterial pressure, and systemic venous pressure. The objective is to determine control inputs that minimize a cost function while ensuring the state variables remain within desired physiological ranges, subject to system dynamics and constraints.

We consider $X^e = (P_{aO_2}^e, P_{aCO_2}^e, P_{as}^e, P_{vs}^e)^t$ as the corresponding steady state vector, and we set $X^* = (P_{aO_2}^*, P_{aCO_2}^*, P_{as}^*, P_{vs}^*)^t$ as the solution of the following optimal problem.

Parameter	Unit	Male	Female
γ_{Q_c}	dl/min	0.5264	0.2667
$\gamma_{Q_{O_2}}$	mL/mmol	0.0054	0.0128
$\gamma_{Q_{CO_2}}$	dl/min	3.2681	1.4704
γ_{MLa}	mmol · L ⁻¹ /mmHg	0.0282	0.0274
γ_{vO_2}	Constant	0.0180	0.0387
γ_{V_E}	L ² mmol ⁻¹ /min	2.4991	2.1011
γ_{aO_2}	Constant	2.5313	2.6769
γ_{aCO_2}	Constant	0.3950	0.3736
T_{Dc}	Constant	0.4248	0.4353
T_{DE}	Constant	3.9997	3.6747
T_{DO_2}	Constant	0.4842	0.2278
k_1	Constant	0.0018	0.0094
k_2	Constant	0.1336	0.0831
α	Constant	0.2336	0.4082
β	Constant	-0.0098	-0.0007

Table 2: Values of estimated parameters.

Find X^* as solution of

$$J(X) = \int_0^{T_{\max}} q_{aO_2} (P_{aO_2} - P_{aO_2}^e)^2 + q_{aCO_2} (P_{aCO_2} - P_{aCO_2}^e)^2 + q_{as} (P_{as} - P_{as}^e)^2 + q_{vs} (P_{vs} - P_{vs}^e)^2 + q_H (H - H^e)^2 + q_{\dot{V}_A} (\dot{V}_A - \dot{V}_A^e), \quad (2)$$

subject to the mathematical model (1). Here, H and \dot{V}_A represent the heart rate and alveolar ventilation, respectively, while q_{aO_2} , q_{aCO_2} , q_{as} , q_{vs} , q_H and $q_{\dot{V}_A}$ denote weighting factors. T_{\max} denotes the maximum allowable duration of the physical activity.

The optimal control strategy is based on the minimization of a quadratic cost function that penalizes both deviations of physiological variables from their equilibrium and the control effort applied. It considers arterial partial pressures of oxygen (P_{aO_2}) and carbon dioxide (P_{aCO_2}), systemic arterial pressure (P_{as}), systemic venous pressure (P_{vs}), as well as the control variables, heart rate (H) and alveolar ventilation (\dot{V}_A).

The weighting coefficients (q_{aO_2} , q_{aCO_2} , q_{as} , q_{vs}) define the relative importance of regulating blood gases and cardiovascular pressures, while q_H and $q_{\dot{V}_A}$ limit excessive control variations to ensure physiologically realistic profiles. The balance between these weightings ensures effective stabilization of pressures and gas exchange while maintaining plausible control actions.

The discretization relies on two complementary parameters. The parameter N denotes the dimension of the vector space spanned by the B-spline basis functions, that is, the number of B-splines used to parameterize the control variables. Each control input is

therefore expressed as a linear combination of these N basis functions. In contrast, M , as defined in relation (6), represents the number of discretization points in \mathbb{R} used for the numerical evaluation of the state equations and the cost functional over the considered time horizon.

To approximate the system described by equations (1), we consider

$$\mathcal{B}^N = \{\psi_j^N, j = 1, \dots, N\},$$

a set of linear B-spline basis functions defined on a uniform grid

$$\Omega_N = \left\{ t_k = \frac{kT_{\max}}{N}, k = 0, \dots, N \right\},$$

such that

$$\psi_i^N(t_k) = \delta_{ik}.$$

In the proposed optimal control framework, the time-dependent control variables, namely the heart rate $H(t)$ and the alveolar ventilation $\dot{V}_A(t)$, are parameterized using cubic B-spline basis functions (order 3). This choice ensures a smooth (C^2 -continuous) representation of the control trajectories, which is physiologically consistent with the gradual nature of cardiovascular and ventilatory adjustments during exercise.

The control horizon $[0, T_{\max}]$, with $T_{\max} = 120$ min, is discretized using a uniform knot sequence with $N = 12$ subintervals. The resulting B-spline basis functions are locally supported, being nonzero only over a limited time span, which allows local modifications of the control profiles without affecting their global structure. The control variables are thus expressed as linear combinations of these basis functions, yielding smooth and flexible trajectories while transforming the continuous-time optimal control problem into a finite-dimensional parameter optimization problem.

The use of cubic B-splines provides an effective compromise between numerical stability and modeling accuracy, enabling adequate smoothing of the control signals while preserving their responsiveness to exercise-induced perturbations. Grid independence was assessed by repeating the simulations using both coarser and finer discretizations (varying the number of control parameters and time nodes), which resulted in negligible changes in the state trajectories and in the value of the cost functional. This confirms the robustness of the numerical discretization and the independence of the results with respect to the chosen grid resolution.

Let us introduce the vector space W^N whose basis is denoted by \mathcal{B}^N . Thus, we have

$$\begin{aligned} \dim W^N &= N, \\ W^N &\subset W^{N+1}. \end{aligned}$$

Let us once again consider $W = C^0(0, T)$, and define the following interpolation operator

$$\begin{aligned} \Pi^N : W &\longrightarrow W^N \\ \phi &\longmapsto \Pi^N \phi. \end{aligned}$$

This meets the following condition

$$\Pi^N \phi(t_k) = \phi(t_k), \quad k = 1, \dots, N.$$

It is straightforward to verify that

$$\|\Pi^N \phi - \phi\|_W \xrightarrow{N \rightarrow \infty} 0, \quad \forall \phi \in W,$$

$$\|\Pi^N\| = \sup_{\substack{\phi \neq 0 \\ \phi \in W}} \frac{\|\Pi^N \phi\|_W}{\|\phi\|_W} = 1.$$

Hence, the system (1) can be approximated as follows. Find $(Q_c^N, Q_{O_2}^N, Q_{CO_2}^N, C_{MLa}^N, C_{vO_2}^N, V_E^N, P_{aO_2}^N, P_{aCO_2}^N, P_{as}^N, P_{vs}^N) \in (W^N)^{10}$ solution of the system:

$$\begin{aligned} \tau_c \frac{dQ_c^N(t)}{dt} &= -Q_c^N(t) + \gamma_{Q_c} C_{vO_2}^N(t) W_r e^{T_{Dc}}, \\ \tau_{O_2} \frac{dQ_{O_2}^N(t)}{dt} &= -Q_{O_2}^N(t) + \gamma_{Q_{O_2}} C_{MLa}^N(t) W_r e^{T_{DO_2}}, \\ \rho \frac{dQ_{CO_2}^N(t)}{dt} &= -Q_{CO_2}^N(t) + \gamma_{Q_{CO_2}} C_{vO_2}^N(t), \\ V_M \frac{dC_{MLa}^N(t)}{dt} &= -C_{MLa}^N(t) + \gamma_{MLa} P_{aO_2}^N(t), \\ \frac{dC_{vO_2}^N(t)}{dt} &= -C_{vO_2}^N(t) + \gamma_{vO_2} Q_{O_2}^N(t) \tag{3} \\ \tau_E \frac{dV_E^N(t)}{dt} &= -V_E^N(t) + \gamma_{V_E} C_{MLa}^N(t) e^{T_{DE}}, \\ \frac{dP_{aO_2}^N(t)}{dt} &= -P_{aO_2}^N(t) + \gamma_{aO_2} P_{aCO_2}^N(t), \\ \frac{dP_{aCO_2}^N(t)}{dt} &= -P_{aCO_2}^N(t) + \gamma_{aCO_2} P_{aO_2}^N(t), \\ \frac{dP_{as}^N(t)}{dt} &= -P_{as}^N(t) + (P_{vs}^N)^\alpha(t) f_1^N(H(t)), \\ \frac{dP_{vs}^N(t)}{dt} &= -P_{vs}^N(t) + (P_{as}^N)^\beta(t) f_2^N(\dot{V}_A(t)), \end{aligned}$$

Parameter	Description	Unit	Value	Source
τ_c	Response time of the cardiac output	Second (s)	19	[9]
W_τ	Work rate	Watt (W)	75	[10]
τ_{O_2}	Response time of oxygen consumption	Second (s)	182	[9]
ρ	Linear constant related to carbon dioxide production	Constant	50	[9]
τ_E	Response time of the control of ventilation	Second(s)	53	[9]
V_M	Effective volume of lactate in the muscle compartment	Litre (L)	8.1	[9]
IRV(Male)	Inspiratory reserve volume	Milliliter (mL)	3,000	[10]
IRV(Female)	Inspiratory reserve volume	Milliliter (mL)	2,100	[10]
ERV(Male)	Expiration reserve volume	Milliliter (mL)	1,100	[10]
ERV(Female)	Expiration reserve volume	Milliliter (mL)	800	[10]
Q	Cardiac output	$L \cdot \text{min}^{-1}$	6	[11]
R_s	Peripheral resistance in the systemic circuit	mmHg · min/L	14.6	[10]
VD	Volume of dead space	Milliliter (mL)	150	[10]

Table 3: Description and values of parameters from the literature.

with

$$\begin{aligned}
 Q_c^N(0) &= Q_{c,0}^N, & Q_{O_2}^N(0) &= Q_{O_2,0}^N, \\
 Q_{CO_2}^N(0) &= Q_{CO_2,0}^N, & C_{MLa}^N(0) &= C_{MLa,0}^N, \\
 C_{vO_2}^N(0) &= C_{vO_2,0}^N, & V_E^N(0) &= V_{E,0}^N, \\
 P_{aO_2}^N(0) &= P_{aO_2,0}^N, & P_{aCO_2}^N(0) &= P_{aCO_2,0}^N, \\
 P_{as}^N(0) &= P_{as,0}^N, & P_{vs}^N(0) &= P_{vs,0}^N,
 \end{aligned}$$

such that

$$\begin{aligned}
 |Q_{c,0} - Q_{c,0}^N| &\xrightarrow{N \rightarrow \infty} 0, & |C_{MLa,0} - C_{MLa,0}^N| &\xrightarrow{N \rightarrow \infty} 0, \\
 |Q_{CO_2,0} - Q_{CO_2,0}^N| &\xrightarrow{N \rightarrow \infty} 0, & |Q_{O_2,0} - Q_{O_2,0}^N| &\xrightarrow{N \rightarrow \infty} 0, \\
 |C_{vO_2,0} - C_{vO_2,0}^N| &\xrightarrow{N \rightarrow \infty} 0, & |V_{E,0} - V_{E,0}^N| &\xrightarrow{N \rightarrow \infty} 0, \\
 |P_{aO_2,0} - P_{aO_2,0}^N| &\xrightarrow{N \rightarrow \infty} 0, & |P_{vs,0} - P_{vs,0}^N| &\xrightarrow{N \rightarrow \infty} 0, \\
 |P_{as,0} - P_{as,0}^N| &\xrightarrow{N \rightarrow \infty} 0, & |P_{aCO_2,0} - P_{aCO_2,0}^N| &\xrightarrow{N \rightarrow \infty} 0.
 \end{aligned}$$

The following approach is used to discretize the optimal problem (2):

$$\begin{aligned}
 \min_{\lambda \in Q} J^N(\lambda) &= \int_0^{T_f} \left(q_{aO_2} (P_{aO_2}^N - P_{aO_2}^e)^2 \right. & (4) \\
 &+ q_{aCO_2} (P_{aCO_2}^N - P_{aCO_2}^e)^2 \\
 &+ q_{as} (P_{as}^N - P_{as}^e)^2 + q_{vs} (P_{vs}^N - P_{vs}^e)^2 \\
 &+ q_H (H^N - H^e)^2 + q_{\dot{V}_A} (\dot{V}_A^N - \dot{V}_A^e)^2 \Big) dt.
 \end{aligned}$$

We seek

$$\lambda^M = \left(H^N - H^e, \dot{V}_A^N - \dot{V}_A^e \right)^t \in Q^M,$$

which is an approximated solution of (4) within the set $Q^M = (W^M)^2$ such that

$$\lambda_j^M = \sum_{k=0}^M \lambda_{j,k}^M \psi_k(t), \quad j = 1, 2.$$

Consequently, the cost function (4) takes the following form

$$\begin{aligned}
 J^N(\lambda^M) &\approx \sum_{k=1}^M \left(q_{aO_2} (P_{aO_2}^N(t_k) - P_{aO_2}^e)^2 \right. & (5) \\
 &+ \sum_{j=1}^2 q(\lambda_{j,k}^M)^2 + q_{aCO_2} (P_{aCO_2}^N(t_k) - P_{aCO_2}^e)^2 \\
 &+ q_{as} (P_{as}^N(t_k) - P_{as}^e)^2 + q_{vs} (P_{vs}^N(t_k) - P_{vs}^e)^2 \Big) \frac{T_{\max}}{M},
 \end{aligned}$$

where $q = (q_H, q_{\dot{V}_A})^t$. Note that (5) is obtained using the rectangular method, where the discretization is carried out over a regular grid Ω_M .

The discretized version of the cost function (4) is written as follows:

$$J^N(\lambda^M) \approx \Delta t \left((Y^T R Y) + (\lambda^M)^T S \lambda^M \right),$$

where

$$\begin{aligned}
 R &= \begin{pmatrix} q_{aO_2} & 0 & 0 & 0 \\ 0 & q_{aCO_2} & 0 & 0 \\ 0 & 0 & q_{as} & 0 \\ 0 & 0 & 0 & q_{vs} \end{pmatrix}, \\
 S &= \begin{pmatrix} q_H & 0 \\ 0 & q_{\dot{V}_A} \end{pmatrix},
 \end{aligned}$$

and

$$\begin{aligned}
 Y &= \left(P_{aO_2}^N(t_k) - P_{aO_2}^e, P_{aCO_2}^N(t_k) - P_{aCO_2}^e, \right. \\
 &\left. P_{as}^N(t_k) - P_{as}^e, P_{vs}^N(t_k) - P_{vs}^e \right)^t.
 \end{aligned}$$

The weighting matrices R and S in the quadratic cost function were chosen to balance the relative importance between state regulation and control effort. Higher weights were assigned to arterial pressures (P_{as} , P_{vs})

and blood gas variables (P_{aO_2} , P_{aCO_2}) in matrix R , reflecting their primary physiological relevance for homeostasis during exercise. The weights associated with the control variables (heart rate H and alveolar ventilation \dot{V}_A) in matrix S were selected to penalize excessive control actions and ensure smooth and realistic control profiles consistent with physiological limits.

Finally, the optimal control problem (2) subject to (1) is formulated in discrete form as follows.

Find $\lambda^{*,M} \in \mathbb{R}^{(M+1)} \times \mathbb{R}^{(M+1)}$ as a solution of

$$\begin{aligned} & \min_{\lambda^M \in \mathbb{R}^{(M+1)} \times \mathbb{R}^{(M+1)}} J^N(\lambda^M) \\ & \approx \Delta t \left((Y^T R Y) + (\lambda^M)^T S \lambda^M \right), \end{aligned} \quad (6)$$

subject to (3) where λ^M is an $(M + 1) \times 2$ whose components $\lambda_{j,k}^M$ correspond to the functions λ_j^N in \mathcal{B}^N , and Y is the matrix whose $(j, k)^{th}$ component is given by $X_j^N(t_k) - X_k^e$.

IV. NUMERICAL SIMULATION

Table 4 outlines the initial values used in the mathematical model developed to simulate the cardiovascular-respiratory system during exercise in Chad.

The initial values in the Table 4 represent baseline physiological conditions, including heart rate, blood pressure, oxygen and carbon dioxide concentrations, lung volume, and blood flow rates. Each parameter is chosen based on clinical data relevant to the target population, ensuring realistic model behavior. These initial conditions serve as the foundation for simulating dynamic responses to exercise, enabling the model to predict how blood and gas pressures are regulated to maintain homeostasis under varying levels of physical activity in the given environment.

For both exercise types (moderate and intense), the initial values of the controls of cardiovascular-respiratory system, heart rate (H) and alveolar ventilation (\dot{V}_A), are assumed as 70 beats per minute and $6 \text{ L} \cdot \text{min}^{-1}$, respectively. The values that represent steady-state physiological conditions under resting or controlled activity levels are shown in the Table 5.

Physiological bounds were imposed on the control variables according to exercise data, namely $60 \leq H \leq 180 \text{ bpm}$ and $4 \leq \dot{V}_A \leq 30 \text{ L} \cdot \text{min}^{-1}$. Throughout all simulations, optimal controls remained within these admissible ranges, and the constraints were not saturated, indicating that they were not active. This confirms that the computed controls stayed within physiologically sound limits while successfully achieving pressure stabilization.

Variable	Male	Female
Q_c	4.5	4.2
Q_{O_2}	4.1	3.5
Q_{CO_2}	0.18	0.16
C_{MLa}	0.9	0.8
C_{vO_2}	0.14	0.14
V_E	6.1	5.3
P_{aO_2}	90	90
P_{aCO_2}	38	38
P_{as}	80	70
P_{vs}	3.9	3.9

Table 4: Initial conditions of the mathematical model.

The Table 6 presents the weights (Components of the matrices S and R) taken for solving the optimal control problem (6) subject to the constraints (3).

Tables 7 and 8 present the prediction errors of the simulated variables in terms of RMSE and MAE for different profiles, including distinctions by sex (male/female) and exercise intensity levels. These results provide an assessment of the accuracy and robustness of the model in reproducing the observed physiological responses.

Sex-related differences were quantified from the steady-state values reported in Table 5. During moderate exercise, females exhibit a higher heart rate ($\Delta H = +5 \text{ bpm}$), combined with a lower alveolar ventilation ($\Delta \dot{V}_A = -1.8 \text{ L} \cdot \text{min}^{-1}$), reduced systemic arterial pressure ($\Delta P_{as} = -5 \text{ mmHg}$), and slightly lower systemic venous pressure ($\Delta P_{vs} = -0.5 \text{ mmHg}$). In parallel, a small decrease in arterial carbon dioxide pressure is observed ($\Delta PaCO_2 = -0.5 \text{ mmHg}$), while arterial oxygen pressure remains slightly higher ($\Delta PaO_2 = +2 \text{ mmHg}$). Under intense exercise, the heart rate difference persists ($\Delta H = +5 \text{ bpm}$) and the ventilatory difference increases ($\Delta \dot{V}_A = -3 \text{ L} \cdot \text{min}^{-1}$), whereas systemic arterial and venous pressures ($\Delta P_{as} = 0$, $\Delta P_{vs} = -0.5 \text{ mmHg}$) as well as $PaCO_2$ become globally comparable between sexes. These results highlight sex-specific cardiovascular-respiratory control strategies, consistent with differentiated physiological adaptations to exercise.

These parameters include stable blood and gas pressures, heart rate, and alveolar ventilation. The equilibrium values ensure that the model accurately reflects the body's ability to maintain homeostasis, serving as a reference point for analyzing deviations caused by varying exercise intensities and environmental factors.

The numerical results for the male case, depicted in Figures 1, 2, 3, are obtained by addressing the optimal control problem defined in (6) while adhering

Parameters	Moderate exercise		Intense exercise	
	Male	Female	Male	Female
He	110	115	145	150
\dot{V}_{Ae}	9	7.2	20	17
P_{aO_2e}	95	97	100	99
P_{aCO_2e}	36	35.5	35	35
P_{ase}	115	110	120	120
P_{vse}	3	2.5	2.5	2

Table 5: Value of parameters at equilibrium states during exercise.

Param. weights	Moderate exercise		Intense exercise	
	Male	Female	Male	Female
q_H	10^8	10^9	10^9	10^8
$q_{\dot{V}_A}$	10^8	10^9	10^8	10^8
q_{aO_2}	10^8	10^9	10^9	10^7
q_{aCO_2}	10^8	10^8	10^9	10^8
q_{as}	10^8	10^8	10^8	10^7
q_{vs}	10^8	10^9	10^9	10^8

Table 6: Weights associated with the variables of the cost function for optimization.

to the constraints specified in (3). These figures illustrate the system’s behavior under optimal conditions, highlighting the effectiveness of the control strategy in regulating blood and gas pressure dynamics within the cardiovascular-respiratory model during exercise, as designed for maintaining physiological homeostasis in the studied male population.

Similarly, Figures 4, 5, and 6 highlight the effectiveness of the control strategy in regulating blood and gas pressure dynamics within the cardiovascular-respiratory model during exercise for the female case. These results demonstrate the model’s ability to maintain physiological homeostasis, as designed, but now applied to the studied female population.

V. DISCUSSION OF RESULTS

Figure 1 presents the dynamic response of heart rate (curves a and b) and alveolar ventilation (curves c and d) for male during exercise. Under moderate exercise (curves (a) and (c)), both heart rate and ventilation increase progressively before stabilizing at a plateau, indicating the achievement of a new physiological equilibrium where oxygen supply meets muscular demand. In contrast, intense exercise (curves (b) and (d)) triggers a more rapid and pronounced rise in both parameters, consistent with cardiovascular-respiratory physiology, which explains that higher metabolic activity requires increased cardiac output and pulmonary ventilation to maintain oxygen delivery and carbon dioxide (CO_2)

Parameters	Moderate exercise		Intense exercise	
	Male	Female	Male	Female
P_{aO_2}	2.48	1.63	3.44	3.33
P_{aCO_2}	0.73	0.64	1.7	1.07
P_{as}	3.16	2.45	4.87	3.96
P_{vs}	0.93	0.79	0.78	0.93

Table 7: RMSE values are reported for the four physiological pressure variables (P_{aO_2} , P_{aCO_2} , P_{as} , P_{vs}).

Parameters	Moderate exercise		Intense exercise	
	Male	Female	Male	Female
P_{aO_2}	2.42	1.1	3.43	3.1
P_{aCO_2}	0.68	0.49	1.68	0.99
P_{as}	3.2	3.38	3.08	3.23
P_{vs}	0.94	0.6	0.64	0.48

Table 8: MAE values are reported for the four physiological pressure variables (P_{aO_2} , P_{aCO_2} , P_{as} , P_{vs}).

clearance. For female (Figure 4), similar trends are observed, but alveolar ventilation reaches higher values than in men under both exercise intensities. This enhanced ventilatory response may be attributed to sex-related physiological differences, such as smaller lung volumes, higher respiratory rates, and hormonal influences like estrogen, which affect ventilatory control and sensitivity during physical exertion.

Figure 2 illustrates the variations in arterial oxygen pressure (curves (a) and (b)) and arterial carbon dioxide pressure (curves (c) and (d)) for male during exercise. Under moderate effort (curves (a) and (c)), P_{aO_2} shows a slight increase before stabilizing, while P_{aCO_2} decreases moderately, indicating that ventilation effectively adapts to meet metabolic demands. In intense exercise (curves (b) and (d)), P_{aO_2} remains elevated and P_{aCO_2} drops more significantly, reflecting hyperventilation, a physiological response to increased carbon dioxide production and oxygen consumption. According to respiratory physiology, this mechanism enhances gas exchange efficiency and helps maintain acid-base balance. In female (Figure 5), P_{aO_2} (curves (a) and (b)) remains slightly higher than in men, while P_{aCO_2} (curves (c) and (d)) decreases at a similar or slightly faster rate. This suggests that female may exhibit more efficient pulmonary gas exchange, potentially due to higher respiratory rates and greater ventilatory responsiveness during physical activity.

Figures 3 and 6 illustrate the behavior of systemic arterial pressure (P_{as} , curves (a) and (b)) and systemic venous pressure (P_{vs} , curves c and d) during exercise. In men, moderate exercise (curves a and c) leads to

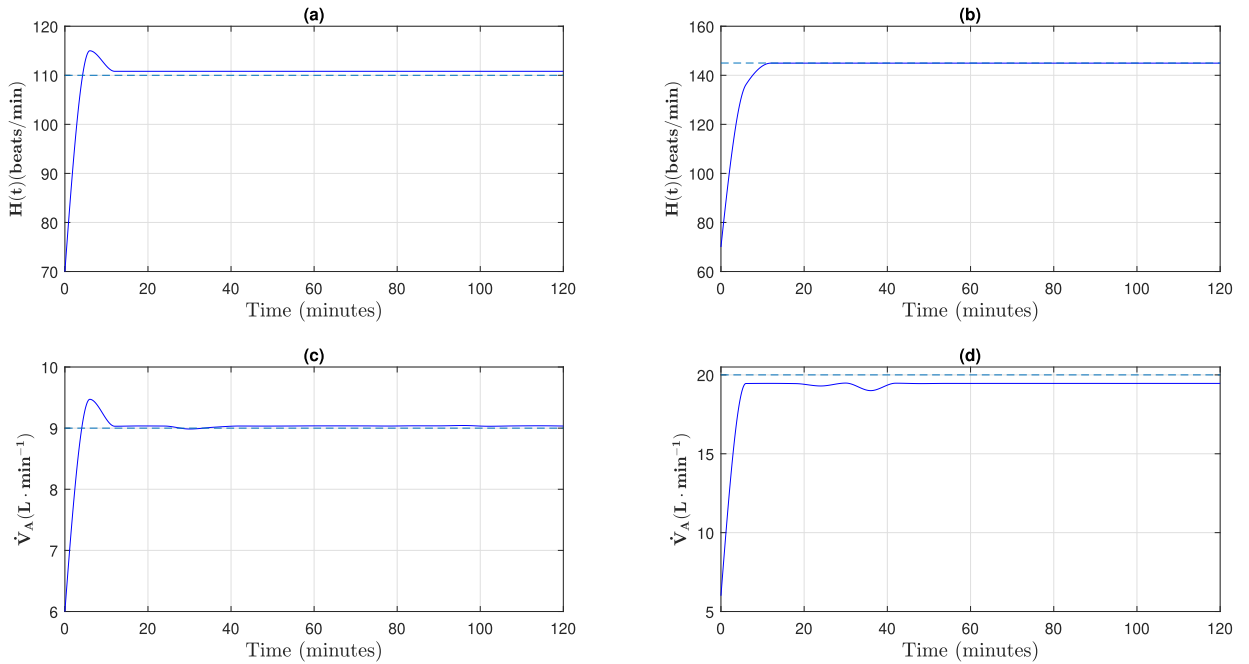


Fig. 1: Evolution of heart rate and alveolar ventilation for male during moderate (curves a and c) and intense (curves b and d) exercise.

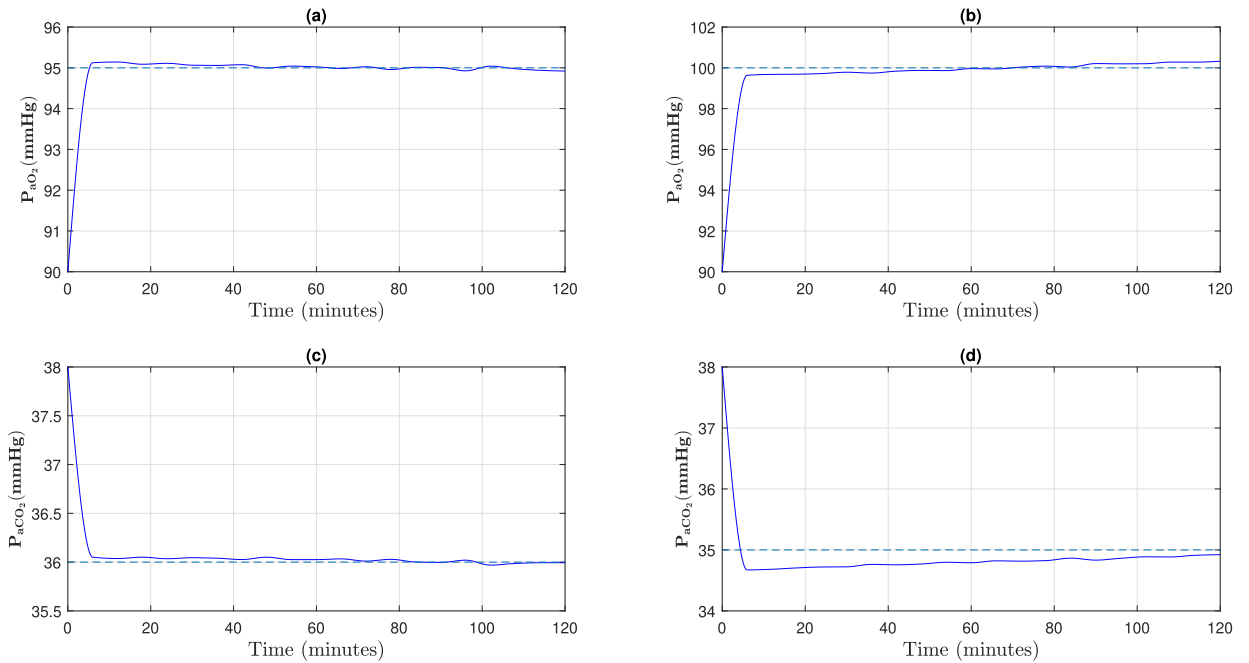


Fig. 2: Evolution of PaO_2 and $PaCO_2$ for male during moderate (curves a and c) and intense (curves b and d) exercise.

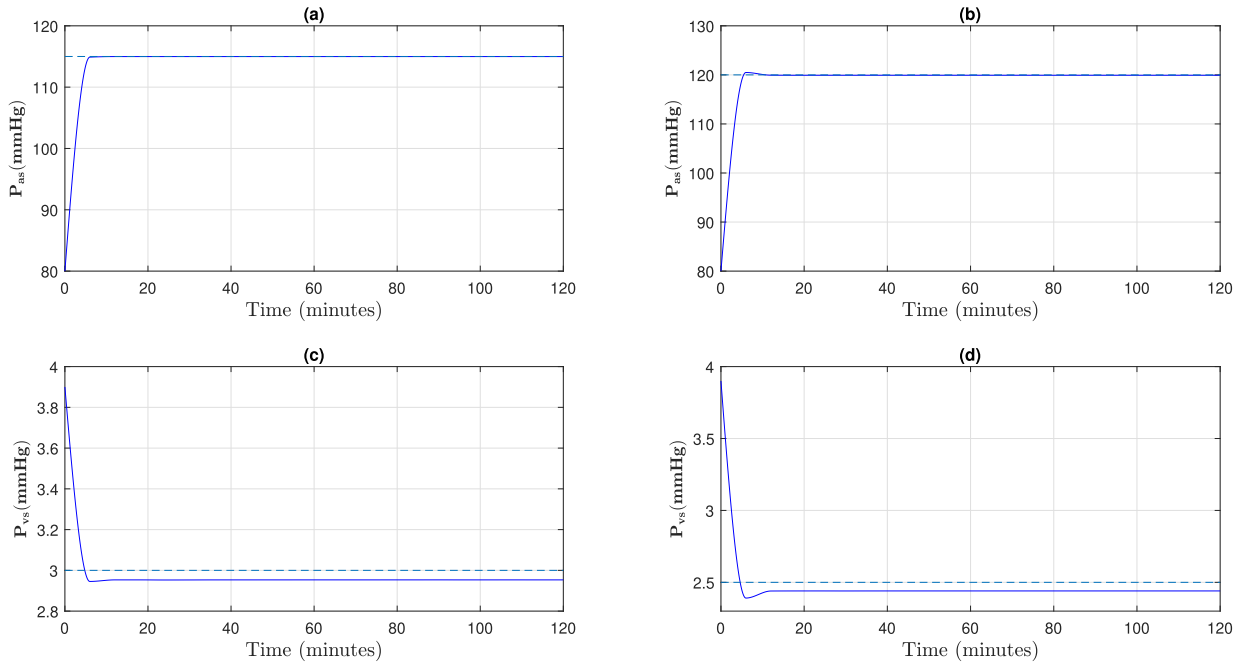


Fig. 3: Evolution of P_{as} and P_{vs} for male during moderate (curves a and c) and intense (curves b and d) exercise.

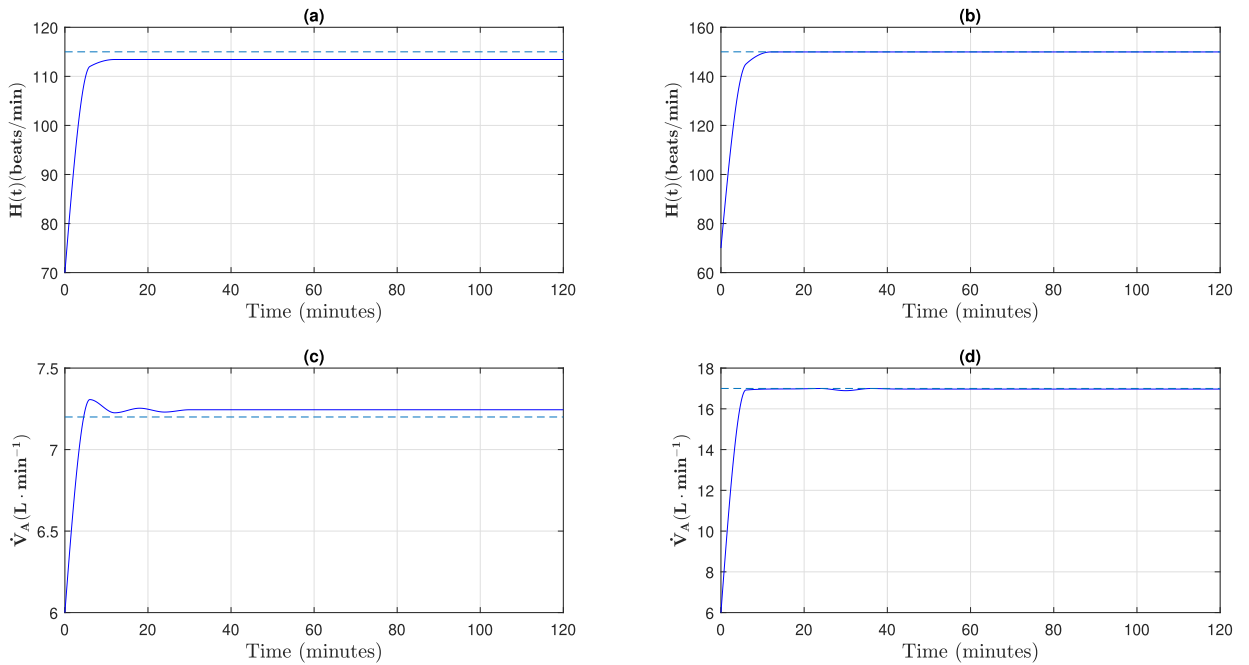


Fig. 4: Evolution of heart rate and alveolar ventilation for female during moderate (curves a and c) and intense (curves b and d) exercise.

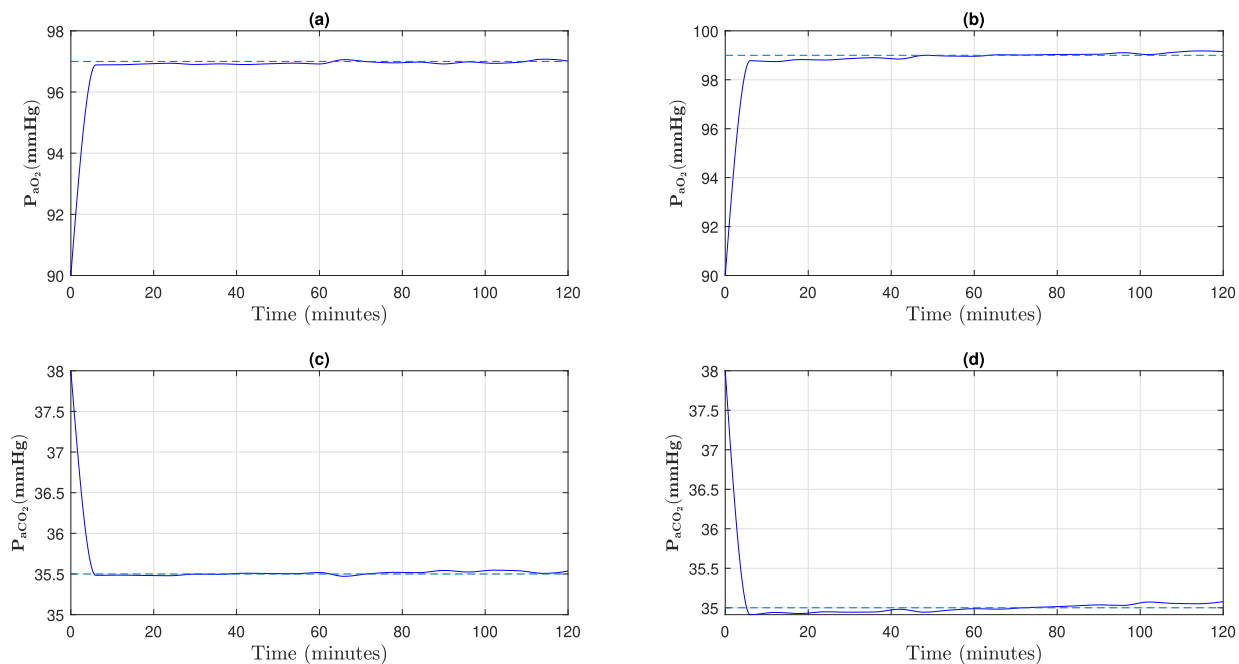


Fig. 5: Evolution of P_{aO_2} and P_{aCO_2} for female during moderate (curves a and c) and intense (curves b and d) exercise.

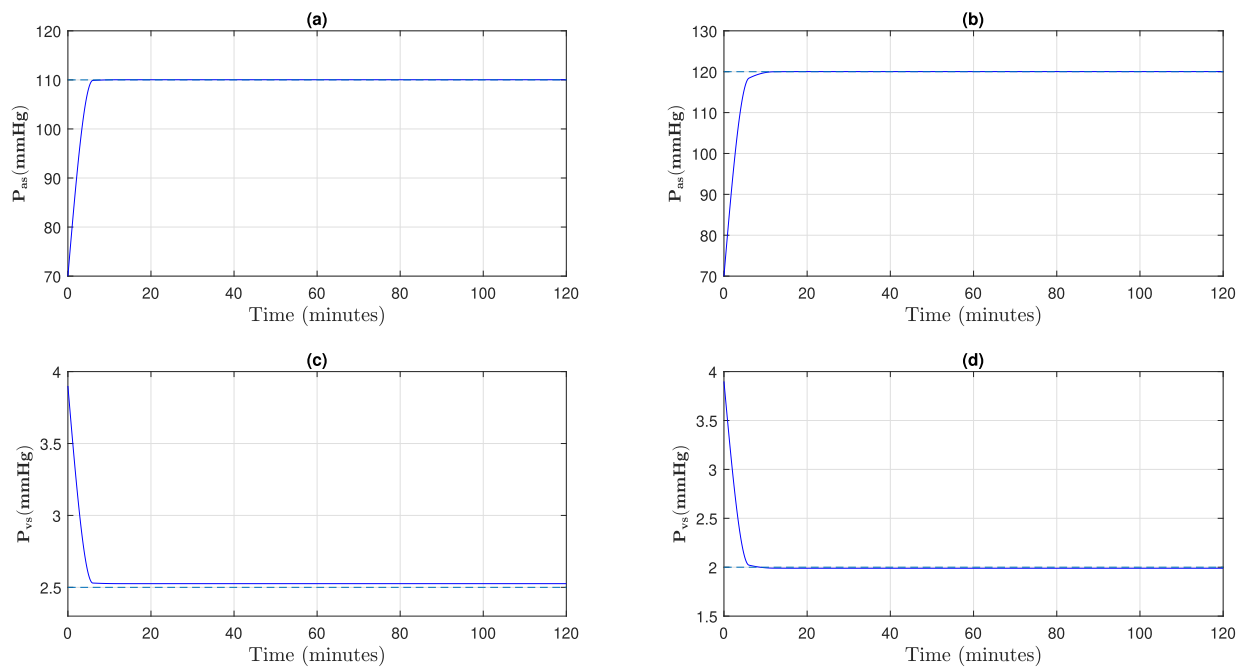


Fig. 6: Evolution of P_{as} and P_{vs} for female during moderate (curves a and c) and intense (curves b and d) exercise.

a gradual rise in P_{as} and a slow decrease in systemic venous pressure (P_{vs}), indicating a well-regulated cardiovascular response to increased demand. During intense exercise (curves (b) and (d)), P_{as} increases more sharply and stabilizes at higher levels, while P_{vs} drops further. This reflects enhanced venous return, vasoconstriction in non-active regions, and effective redistribution of blood flow toward working muscles, key mechanisms in cardiovascular physiology for maintaining perfusion pressure and oxygen delivery during exertion.

For female (Figure 6), the rise in P_{as} and the fall in P_{vs} are even more pronounced, suggesting a more robust hemodynamic adaptation. This may be influenced by sex-specific cardiovascular regulation, such as differences in vascular tone, hormonal modulation, and cardiac output response.

VI. CONCLUDING REMARKS

This study developed a comprehensive mathematical model integrating the cardiovascular and respiratory systems to regulate blood and gas pressure dynamics during physical exercise, tailored to the physiological characteristics of the Chadian population. By using heart rate and alveolar ventilation as control variables, the model effectively captured the physiological responses seen in trained individuals under both moderate and intense exercise conditions.

The simulation results confirmed the model's ability to replicate key changes in systemic and venous pressures, as well as arterial oxygen and carbon dioxide partial pressures, aligning with known physiological mechanisms of homeostatic regulation.

Notably, the analysis revealed sex-specific differences, with women exhibiting a stronger ventilatory response, an insight that supports the need for personalized or sex-specific modeling. Furthermore, the model demonstrates strong potential as a predictive tool for assessing cardiovascular-respiratory performance during exercise in diverse populations. It offers a foundation for clinical applications aimed at improving cardiorespiratory health and performance in both medical and athletic contexts.

Nonetheless, further refinement and validation against experimental or clinical data are necessary to improve the model's accuracy, adaptability, and practical implementation across broader physiological and environmental conditions. Future work will focus on refining the model's accuracy and expanding its applicability through clinical validation and integration with real-world physiological data.

LIMITATIONS

This study is based on simulations and analyses performed around reference physiological conditions, with measurements mainly evaluated near equilibrium states. While this approach is consistent with the explanatory objective of the model, it limits the detailed analysis of transient cardiovascular-respiratory dynamics under rapid or unanticipated perturbations.

In addition, parameter uncertainty, identifiability, and sensitivity were not formally assessed (e.g., via confidence intervals, bootstrap methods, or sensitivity analysis), which may restrict the evaluation of the relative influence of individual model parameters on the system outputs. Finally, exogenous inputs such as environmental conditions or neuro-hormonal regulatory mechanisms are not explicitly incorporated into the model. These aspects will be addressed in future studies.

ACKNOWLEDGEMENTS

The first author gratefully acknowledges the support and guidance provided by the faculty of the University of N'Djamena throughout this research.

CONFLICT OF INTEREST

The authors declare that there is no conflict of interest regarding the publication of this paper. All research was conducted independently, without any financial, commercial, or personal relationships that could influence the results or interpretations presented in this study.

REFERENCES

- [1] C. A. Sarmiento, A. M. Hernández, L. Y. Serna, M. Á. Mañanas, An integrated mathematical model of the cardiovascular and respiratory response to exercise: model-building and comparison with reported models, *American Journal of Physiology-Heart and Circulatory Physiology*, 320:H1235–H1260, 2021.
- [2] E. Magosso, M. Ursino, Cardiovascular response to dynamic aerobic exercise: A mathematical model, *Medical and Biological Engineering and Computing*, 40:660–674, 2002.
- [3] L. Cheng, O. Ivanova, H.-H. Fan, M. C. K. Khoo, An integrative model of respiratory and cardiovascular control in sleep-disordered breathing, *Respiratory Physiology & Neurobiology*, 174:4–28, 2010.
- [4] H. T. Milhorn Jr., R. Benton, R. Ross, A. C. Guyton, A Mathematical Model of the Human Respiratory Control System, *Biophysical Journal*, 5:27–46, 1965.
- [5] L. M. Ellwein, S. R. Pope, A. Xie, J. J. Batzel, C. T. Kelley, M. S. Olufsen, Patient-specific modeling of cardiovascular and respiratory dynamics during hypercapnia, *Mathematical Biosciences*, 241:56–74, 2013.
- [6] J. J. Batzel, F. Kappel, D. Schneditz, H. T. Tran, Cardiovascular and Respiratory Systems: Modeling, Analysis, and Control, In: *Cardiovascular and Respiratory Systems*, Frontiers in Applied Mathematics, pp. 241–274, 2007.
- [7] J. J. Batzel, M. Bachar, F. Kappel, *Mathematical Modeling and Validation in Physiology: Applications to the Cardiovascular and Respiratory Systems*, Lecture Notes in Mathematics, 2064, Springer, 2012.

- [8] World Health Organization, Noncommunicable Diseases Progress Monitor 2022, <https://www.who.int/publications/item/9789240047761> [24-Mar-2026].
- [9] H. Thamrin, D. J. Murray-Smith, A mathematical model of the human respiratory system during exercise, In: *IASTED International Conference on Modelling, Simulation and Identification (MSI 2009)*, Beijing, China, 12-14 Oct 2009.
- [10] J. M. Ntaganda, J. Niyobuhungiro, W. Banzi, L. Mpinganzima, F. Minani, J. B. Gahutu, V. Dusabejambo, I. Kambutse, Mathematical modelling of human cardiovascular-respiratory system responses to exercise in Rwanda, *International Journal of Mathematical Modelling and Numerical Optimisation*, 9:287–308, 2019.
- [11] S. Timischl, *A global model of the cardiovascular and respiratory system*, Doctoral dissertation, Karl-Franzens-Universität Graz, Austria, 1998.
- [12] Family Practice Notebook: Vital Capacity, [24-Mar-2026], <https://fpnotebook.com/Lung/Lab/VtlCpcty.htm>
- [13] J. D. Melgarejo, W.-Y. Yang, L. Thijs, Y. Li, K. Asayama, T. W. Hansen, et al., Association of Fatal and Nonfatal Cardiovascular Outcomes With 24-Hour Mean Arterial Pressure, *Hypertension*, 77:39–48, 2021.
- [14] K. Wasserman, A. L. Van Kessel, G. G. Burton, Interaction of physiological mechanisms during exercise, *Journal of Applied Physiology*, 22:71–85, 1967.
- [15] B. J. Whipp, H. B. Rossiter, S. A. Ward, Exertional oxygen uptake kinetics: a stamen of stamina?, *Biochemical Society Transactions*, 30:237–247, 2002.
- [16] H. B. Rossiter, S. A. Ward, J. M. Kowalchuk, F. A. Howe, J. R. Griffiths, B. J. Whipp, Dynamic asymmetry of phosphocreatine concentration and O_2 uptake between the on- and off-transients of moderate- and high-intensity exercise in humans, *The Journal of Physiology*, 541:991-1002, 2002.
- [17] B. J. Whipp, H. B. Rossiter, The kinetics of oxygen uptake: Physiological inferences from the parameters, In: *Oxygen Uptake Kinetics in Sport, Exercise and Medicine*, 33 pages, Routledge, 2005.
- [18] K. Wasserman, *Principles of Exercise Testing and Interpretation: Including Pathophysiology and Clinical Applications*, Lippincott Williams & Wilkins, 2005.
- [19] D. R. Bassett, Jr., E. T. Howley, Limiting factors for maximum oxygen uptake and determinants of endurance performance, *Medicine & Science in Sports & Exercise*, 32:70, 2000.
- [20] B. J. Whipp, *The Control of Breathing in Man*, University of Pennsylvania Press, 1987.
- [21] A. P. Fishman, J. A. Elias, *Fishman's Pulmonary Diseases and Disorders*, McGraw-Hill, 1998.
- [22] B. J. Whipp, M. B. Higgenbotham, F. C. Cobb, Estimating exercise stroke volume from asymptotic oxygen pulse in humans, *Journal of Applied Physiology*, 81:2674–2679, 1996.